Energy Minimization in Fluid Flow through Tubes and Networks of Various Geometries

Taha Sochi (Contact: t.sochi@ucl.ac.uk)

London, United Kingdom

Abstract: In this paper we continue our previous investigation about energy minimization in the flow of fluids through tubes and networks of interconnected tubes of various geometries. We will show that the principle of energy minimization holds independent of the geometry of the tubes and networks of such interconnected tubes and independent of the type of fluid in such geometries where in this regard we consider generalized Newtonian fluids. We consider in this investigation the flow of Newtonian fluids through tubes and networks of interconnected tubes of elliptical, rectangular, equilateral triangular and concentric circular annular cross sectional geometries. We also consider a combination of geometric factor with a fluid type factor by showing that the principle of energy minimization holds in the flow of some non-Newtonian fluids (namely power law, Ellis and Ree-Eyring fluids) through tubes and networks of interconnected tubes of elliptical cross sections. The relevance of this study extends beyond tubes and networks of fluid flow to include for instance porous media and electrical networks.[1]

Keywords: Energy minimization, flow in tubes, elliptical tubes, rectangular tubes, triangular tubes, annular tubes, Newtonian fluids, power law fluids, Ellis fluids, Ree-Eyring fluids, rheology, fluid mechanics, fluid dynamics.

[1] All symbols and abbreviations are defined in § Nomenclature in the back of this paper.

Contents

1 Introduction

Optimization is one of the fundamental principles of Nature where physical systems tend to reach their targets through optimizing (usually minimizing) certain physical quantities and attributes. A well known example is Fermat's principle of least time. In particular, energy minimization is a well know principle in many physical systems such as the tendency of excited atomic systems to decay to the lowest available energy levels within certain rules and conditions.

There are quite few investigations on the theoretical formulation and practical application of optimization principles as governing rules that determine the behavior and regulate the design of fluid dynamics systems (see for instance [1–4]). However, we are not aware of the use of optimization principles (and energy minimization in particular) to resolve the pressure fields and obtain flow dynamics quantities and parameters (such as volumetric flow rates) of fluid flow through conduits and networks of interconnected conduits. Yes, a few years ago we have investigated some of these issues (see [5–7]) using energy minimization as a viable principle for resolving the flow fields in conduits and networks as well as a fundamental principle that underlies, and hence explains, the behavior of fluid dynamics systems in general.[2]

In our previous investigations (which we cited already) about energy minimization in the flow of fluids through tubes and networks of interconnected tubes we established that energy minimization principle holds in both cases (i.e. tubes and networks) regardless of the type of fluid (such as Newtonian or power law or Ellis or Ree-Eyring or other types of generalized Newtonian fluids). However, those investigations were limited to tubes of circular (and simply-connected) cross sectional geometry and networks of interconnected circular tubes.

In the present investigation we generalize those results by extending them to some of the most common types of tubes of non-circular (and non-simply-connected) cross sectional geometries and networks of interconnected such tubes. So, we will extend the energy minimization principle to tubes and networks of interconnected tubes of elliptical, rectangular, equilateral triangular and concentric circular annular cross sectional geometries with regard to the flow of Newtonian fluids through these geometries. In addition to this, we will combine non-circular geometry factor with the non-Newtonian fluid factor by extending the principle of energy minimization to the flow of some generalized Newtonian fluids

[2] We should note that variational principles (which we investigated in a number of studies; see for instance [8, 9]) are also optimization principles.

(namely power law, Ellis and Ree-Eyring) through tubes and networks of interconnected tubes of elliptical cross sections.

The result that we will reach in this investigation is that the principle of energy minimization is valid in general, i.e. its validity is independent of the type of fluid and the geometry of conduits (as well as other attributes and characteristics of networks such as their dimensionality and topology). The relevance of the current investigation (as well as our previous investigations) extends beyond the flow of fluids through tubes and networks of interconnected tubes. For example, the principle of energy minimization should similarly apply to the flow of fluids through porous media since porous media are essentially networks of interconnected tubes of irregular geometry and random topology.

In fact, the principle of energy minimization which we establish in this investigation should extend even to networks other than fluid transportation networks. For example, electrical networks of ohmic conductors should also be subject to the energy minimization principle because of the similarity in the fundamental physics between networks of interconnected tubes (for fluid flow) and networks of interconnected ohmic resistors (for electric current flow).

Our plan in this paper (following this introduction) is to prepare the scene for this investigation by providing a general theoretical background about this investigation where we mostly refer to our previous investigations in this regard (see § 2). We then investigate energy minimization principle in the flow of Newtonian fluids through tubes and networks of interconnected tubes of various geometries, i.e. tubes and networks of interconnected tubes of elliptical cross sections, rectangular cross sections, equilateral triangular cross sections, and concentric circular annular cross sections (see § 3). We then investigate energy minimization principle in the flow of three non-Newtonian fluid types (namely power law, Ellis and Ree-Eyring) through tubes and networks of interconnected tubes of elliptical cross sectional geometry (see § 4). The paper is finalized with a list of the main achievements and conclusions of this investigation (see § 5).

2 Theoretical Background and Implementation

The theoretical background of this investigation is largely explained in [5–7] (and [7] in particular). So, in this section we just give an outline or reminder of what have been given already.

The traditional method[3] for resolving the pressure and volumetric flow rate fields in fluid conducting devices is to use the conservation principles, which are normally based on the mass continuity and momentum conservation, in conjunction with the constitutive relations that link the stress to the rate of deformation and are specific to the particular types of fluid employed to model the flow [10–13].

For single conduits, this usually results in an analytical expression that correlates the volumetric flow rate to the applied pressure drop as well as other dependencies on the parameters of the conduits, such as the radius and length of the tube, and the parameters of the fluid such as the shear viscosity and yield stress. For networks of interconnected conduits, the analytical expression for the single conduit for the particular fluid model can be exploited in a numeric solution scheme, which is normally of iterative nature such as the widely used Newton-Raphson procedure for solving a system of simultaneous non-linear equations, in conjunction with the mass conservation principle and the given boundary conditions to obtain the flow fields in the network (see for instance [14, 15]).

The energy minimization method for resolving the pressure and volumetric flow rate fields in fluid conducting devices (which is the foundation of the present investigation as a continuation of the previous investigations of [5–7]) employs a different strategy which will be outlined in the following paragraphs.

The time rate of energy consumption, I, for transporting a certain quantity of fluid through a single conducting device, considering the relevant flow assumptions and conditions, is given by:

$$I = \Delta p \, Q \tag{1}$$

where Δp is the pressure drop across the conducting device and Q is the volumetric flow rate of the transported fluid through the device. For a flow conducting device that consists of or discretized into m conducting elements indexed by l, the total energy consumption rate, I_t, is given by:

[3] We may refer to the results of traditional method by labels like "analytical solutions" or "Poiseuille-type solutions".

$$I_t(p_1, \ldots, p_N) = \sum_{l=1}^{m} \Delta p_l Q_l \tag{2}$$

where N is the number of the boundary and internal nodes. For a single duct, the conducting elements are the discretized sections, while for a network they represent the conducting ducts as well as their discretized sections if discretization is employed.

Starting from randomly selected values for the internal nodal pressure, with the given pressure values for the inlet and outlet boundary nodes, the role of the global multi-variable optimization algorithms in the above-outlined energy consumption model is to minimize the cost function, which is the time rate of the total energy consumption for fluid transportation I_t as given by Eq. 2, by varying the values of the internal nodal pressure while holding the pressure values at the inlet and outlet boundary nodes as constants. The volumetric flow rates, Q, that have to be used in Eq. 2 for the employed fluid models are given by the expressions in Table 1 for Newtonian fluids and Table 6 for non-Newtonian fluids (as will be explained next in § 3 and § 4).

This energy minimization method was implemented using three deterministic global multi-variable optimization algorithms and one stochastic. The deterministic algorithms are: Conjugate Gradient, Nelder-Mead, and Quasi-Newton, while the stochastic is the Global algorithm of Boender *et al.*. For more details about the three employed deterministic algorithms we refer to standard textbooks that discuss these algorithms, while for the Stochastic Global algorithm we refer to [16].[4]

As for single tubes, it is a special case of the forthcoming 1D linear networks of serially connected pipes (see for instance Tables 2 and 7) where all the pipes in the ensemble have the same parameters (such as the semi-major and semi-minor axes for tubes of elliptical cross sections). In this regard all the implemented optimization algorithms produced results which are virtually identical to the analytical solutions for the certain types of fluid as given in Tables 1 and 6.

Regarding the networks, due to the difficulty of presenting the results graphically for the two-dimensional and three-dimensional networks, we present in Figures 2-5 and Figures 6-8 a sample of the results obtained from a range of 1D linear networks (where all the produced results, as we see in the sample, of the traditional method and the energy minimization method are virtually identical). Similar results were obtained from representative samples of 2D and 3D networks of various sizes and topologies (similar to what we did in [7]).

[4] Also see: http://jblevins.org/mirror/amiller/global.txt web page.

3 Newtonian Flow in Various Geometries

In this section we outline our investigation of the flow of Newtonian fluids through tubes and networks of interconnected tubes of elliptical cross sections, rectangular cross sections, equilateral triangular cross sections, and concentric circular annular cross sections (see Figure 1). In this regard we use the analytical expressions of Table 1 (as given for instance in [12, 17]) for the volumetric flow rate of Newtonian fluid flow through these geometries where the coordinate and parametric settings of these geometries with regard to these expressions are illustrated in Figure 1.

We conducted thorough investigations and computations of Newtonian flow through tubes and networks of various dimensionality (i.e. 1D, 2D and 3D) and topology (such as linear, fractals, and irregulars based on cubic and orthorhombic lattices) and of various cross sectional geometries (i.e. elliptical, rectangular, equilateral triangular and concentric circular annular) using Newtonian fluids of various viscosity. All these investigations and computations lead to the definite conclusion that energy minimization holds in all these cases regardless of the type of vessel (i.e. whether single tube or network of interconnected tubes) and its geometry, regardless of the dimensionality and topology of network, and regardless of the viscosity of fluid.

A sample of these investigations and computations for some 1D linear networks (see Tables 2-5) are given in Figures 2-5, i.e. Figure 2 for the flow of a Newtonian fluid through elliptical geometry, Figure 3 for the flow of a Newtonian fluid through rectangular geometry, Figure 4 for the flow of a Newtonian fluid through equilateral triangular geometry, and Figure 5 for the flow of a Newtonian fluid through concentric circular annular geometry. The use of 1D linear networks in this sample demonstration is because of the ease of displaying and clarity of showing and interpreting the results of this type of networks which can be easily displayed on 2D plots (as seen in Figures 2-5) and hence they are clearly analyzed and interpreted.

As we see, this representative sample shows that the solutions that we obtained from the employment of the principle of energy minimization are virtually identical to the Poiseuille-type analytical solutions (as outlined in § 2). So, we can conclude with certainty that the principle of energy minimization holds in general (i.e. independent of the type of vessel and its geometry, the dimensionality and topology of network, and the type of Newtonian fluid).

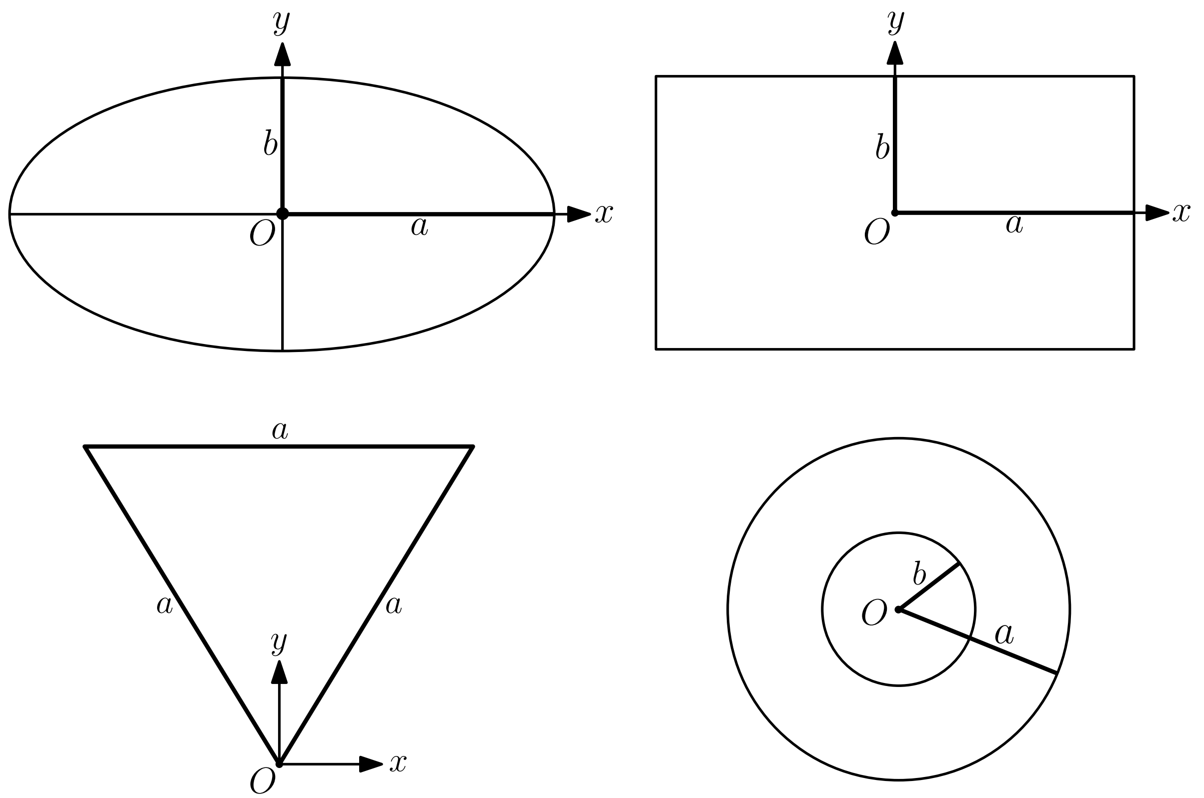

Figure 1: The settings of the elliptical, rectangular, equilateral triangular, and concentric circular annular cross sections of the tubes where O is the origin of coordinates. The z axis is emanating from the origin and is perpendicular to the plane of cross sections. See Table 1 and Table 6.

Table 1: The four cross sectional geometries of tubes and their corresponding volumetric flow rates (Q) for the flow of Newtonian fluids through these tubes. The meanings of the symbols are given in § Nomenclature with reference to Figure 1. See [12, 17].

Geometry of Cross Section	**Volumetric Flow Rate (Q)**
Ellipse	$Q = \frac{\partial p}{\partial z} \frac{\pi a^3 b^3}{4\mu(a^2+b^2)}$
Rectangle	$Q = \frac{\partial p}{\partial z} \frac{4a^3 b}{3\mu} \left[1 - \frac{192a}{\pi^5 b} \sum_{i=1,3,5,\ldots}^{\infty} \frac{\tanh\left(\frac{i\pi b}{2a}\right)}{i^5} \right]$
Equilateral Triangle	$Q = \frac{\partial p}{\partial z} \frac{\sqrt{3}\, a^4}{320\mu}$
Concentric Circular Annulus	$Q = \frac{\partial p}{\partial z} \frac{\pi}{8\mu} \left[a^4 - b^4 - \frac{\left(a^2-b^2\right)^2}{\ln(a/b)} \right]$

Table 2: The semi-major axes a, semi-minor axes b and lengths L of the seven elliptical tubes of the 1D linear network of Figure 2 as well as the pressure drops Δp across them. All numbers are in SI units (i.e. meters and pascals).

a	0.025, 0.021, 0.018, 0.013, 0.017, 0.026, 0.016
b	0.018, 0.019, 0.015, 0.011, 0.014, 0.018, 0.012
L	0.8, 0.6, 0.7, 0.9, 0.9, 0.5, 0.6
Δp	127.62, 116.04, 299.07, 1367.19, 495.96, 74.72, 519.40

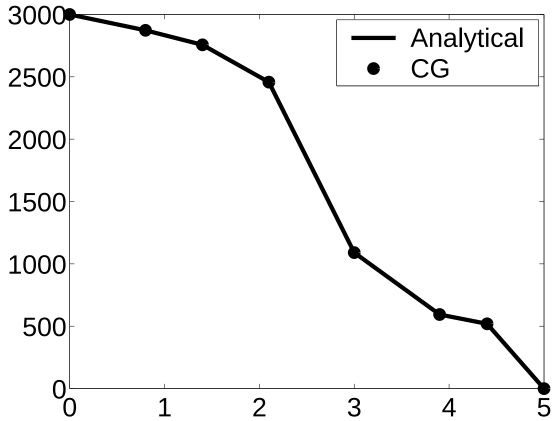

(a) Conjugate Gradient.

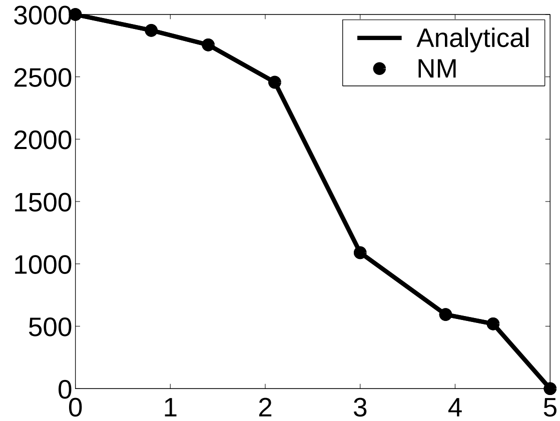

(b) Nelder-Mead.

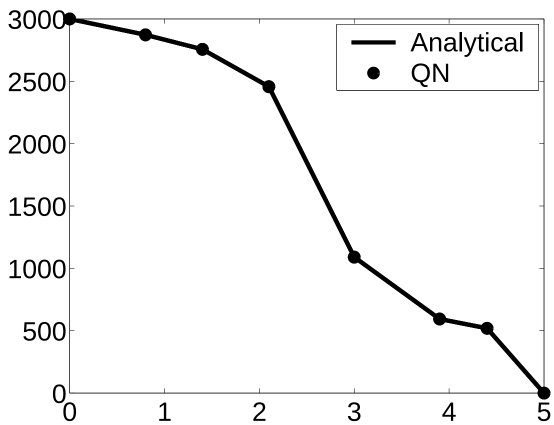

(c) Quasi-Newton.

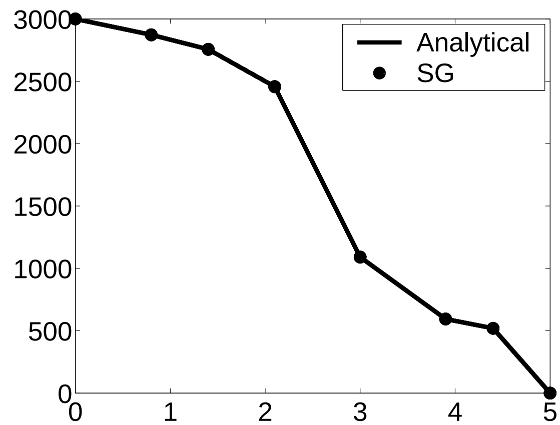

(d) Stochastic Global.

Figure 2: Comparison between the analytical solution and the solutions obtained from the indicated global optimization algorithms which are based on the energy minimization principle for the flow of a Newtonian fluid with $\mu = 0.05$ Pa.s. The computations were carried out using the 1D linear elliptical network of Table 2 with inlet and outlet pressures of 3000 Pa and 0 Pa respectively. The volumetric flow rate through the network is 0.00024061 $m^3.s^{-1}$. In all four sub-figures, the vertical axis represents the network axial pressure in Pa while the horizontal axis represents the network axial coordinate in m.

Table 3: The semi-lengths a, semi-widths b and lengths L of the eight rectangular tubes of the 1D linear network of Figure 3 as well as the pressure drops Δp across them. All numbers are in SI units (i.e. meters and pascals).

a	0.19, 0.17, 0.21, 0.20, 0.22, 0.16, 0.18, 0.23
b	0.12, 0.15, 0.13, 0.14, 0.10, 0.15, 0.16, 0.09
L	1.1, 0.6, 0.8, 0.6, 1.1, 0.7, 1.3, 0.8
Δp	425.29, 169.92, 217.50, 148.25, 539.86, 222.61, 288.39, 488.19

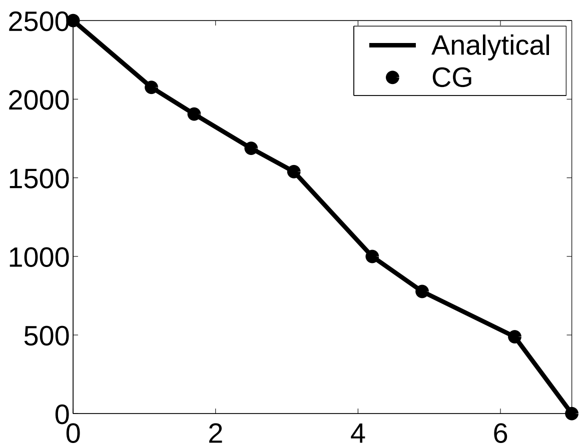

(a) Conjugate Gradient.

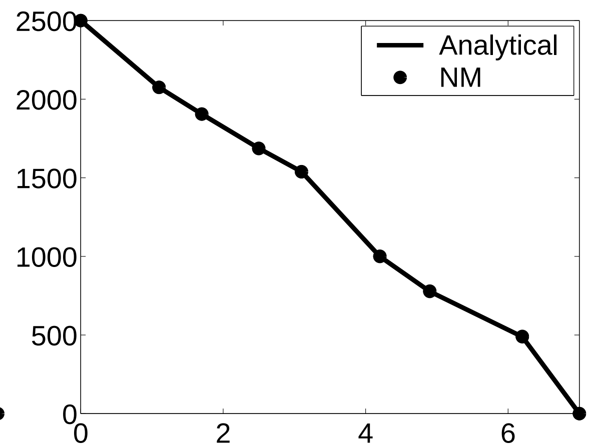

(b) Nelder-Mead.

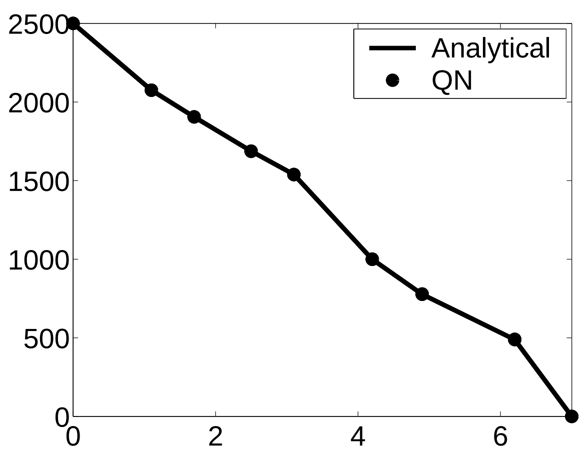

(c) Quasi-Newton.

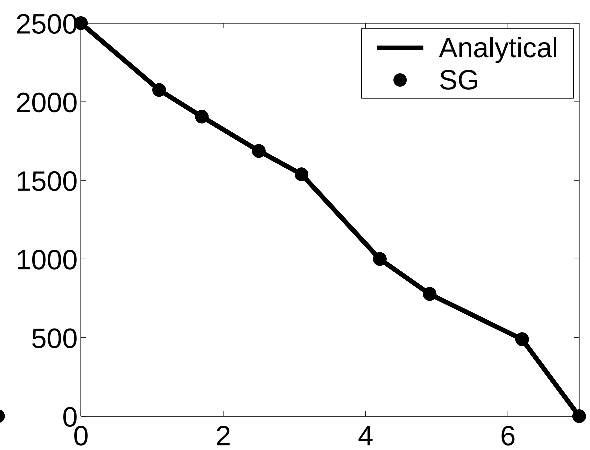

(d) Stochastic Global.

Figure 3: Comparison between the analytical solution and the solutions obtained from the indicated global optimization algorithms which are based on the energy minimization principle for the flow of a Newtonian fluid with $\mu = 0.13$ Pa.s. The computations were carried out using the 1D linear rectangular network of Table 3 with inlet and outlet pressures of 2500 Pa and 0 Pa respectively. The volumetric flow rate through the network is 0.790778 $m^3.s^{-1}$. In all four sub-figures, the vertical axis represents the network axial pressure in Pa while the horizontal axis represents the network axial coordinate in m.

Table 4: The side lengths a and lengths L of the eight equilateral triangular tubes of the 1D linear network of Figure 4 as well as the pressure drops Δp across them. All numbers are in SI units (i.e. meters and pascals).

a	0.019, 0.015, 0.021, 0.014, 0.022, 0.015, 0.018, 0.009
L	0.120, 0.070, 0.080, 0.060, 0.080, 0.060, 0.110, 0.070
Δp	78.83, 118.38, 35.22, 133.72, 29.24, 101.47, 89.71, 913.43

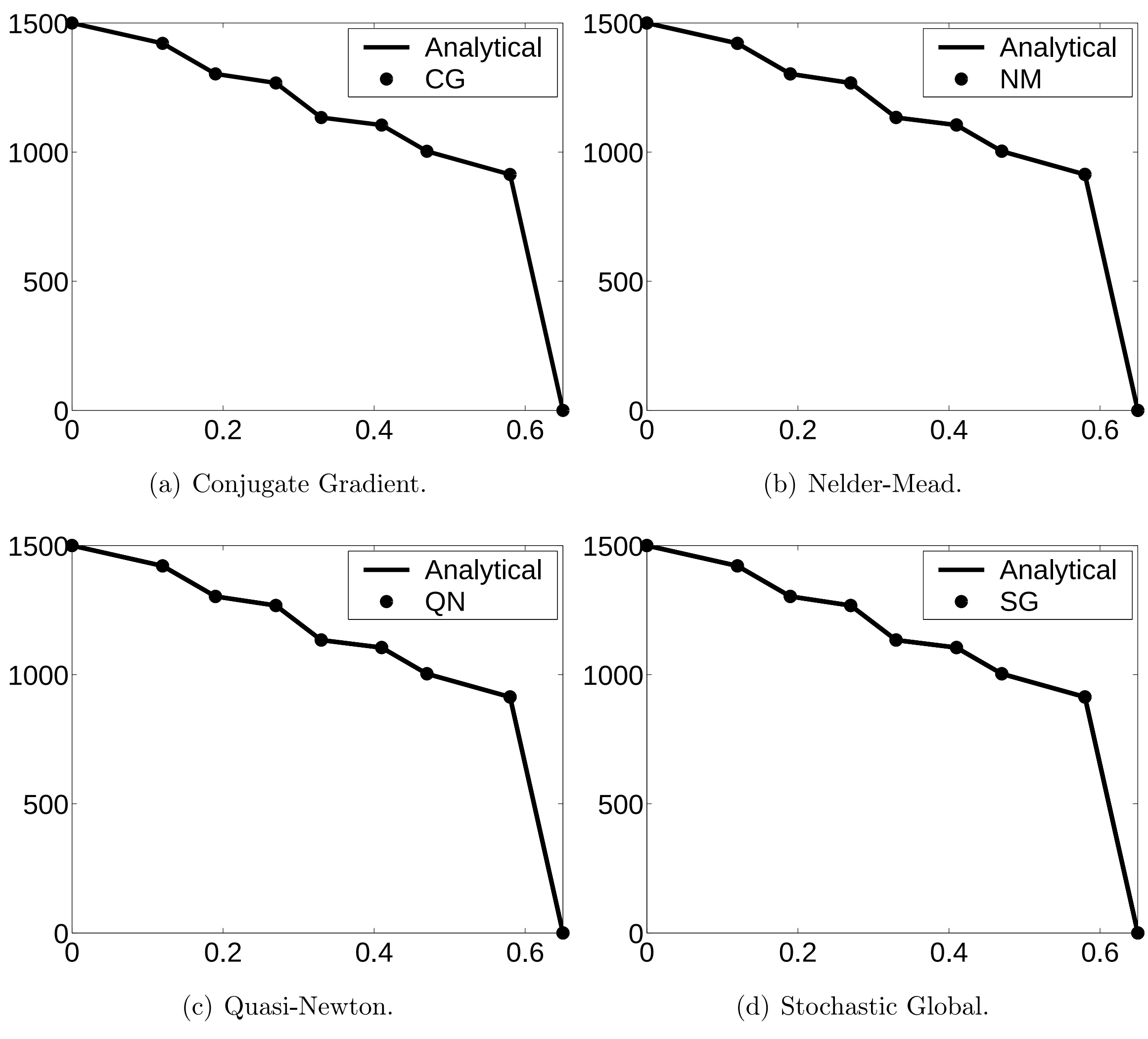

(a) Conjugate Gradient.

(b) Nelder-Mead.

(c) Quasi-Newton.

(d) Stochastic Global.

Figure 4: Comparison between the analytical solution and the solutions obtained from the indicated global optimization algorithms which are based on the energy minimization principle for the flow of a Newtonian fluid with $\mu = 0.1$ Pa.s. The computations were carried out using the 1D linear triangular network of Table 4 with inlet and outlet pressures of 1500 Pa and 0 Pa respectively. The volumetric flow rate through the network is 4.634×10^{-6} $m^3.s^{-1}$. In all four sub-figures, the vertical axis represents the network axial pressure in Pa while the horizontal axis represents the network axial coordinate in m.

Table 5: The outer radii a, inner radii b and lengths L of the seven concentric circular annular tubes of the 1D linear network of Figure 5 as well as the pressure drops Δp across them. All numbers are in SI units (i.e. meters and pascals).

a	0.050, 0.044, 0.052, 0.041, 0.056, 0.040, 0.051
b	0.045, 0.033, 0.039, 0.035, 0.041, 0.030, 0.043
L	0.61, 0.96, 0.88, 1.01, 0.77, 1.12, 0.95
Δp	623.80, 113.62, 53.39, 746.97, 28.52, 194.07, 239.63

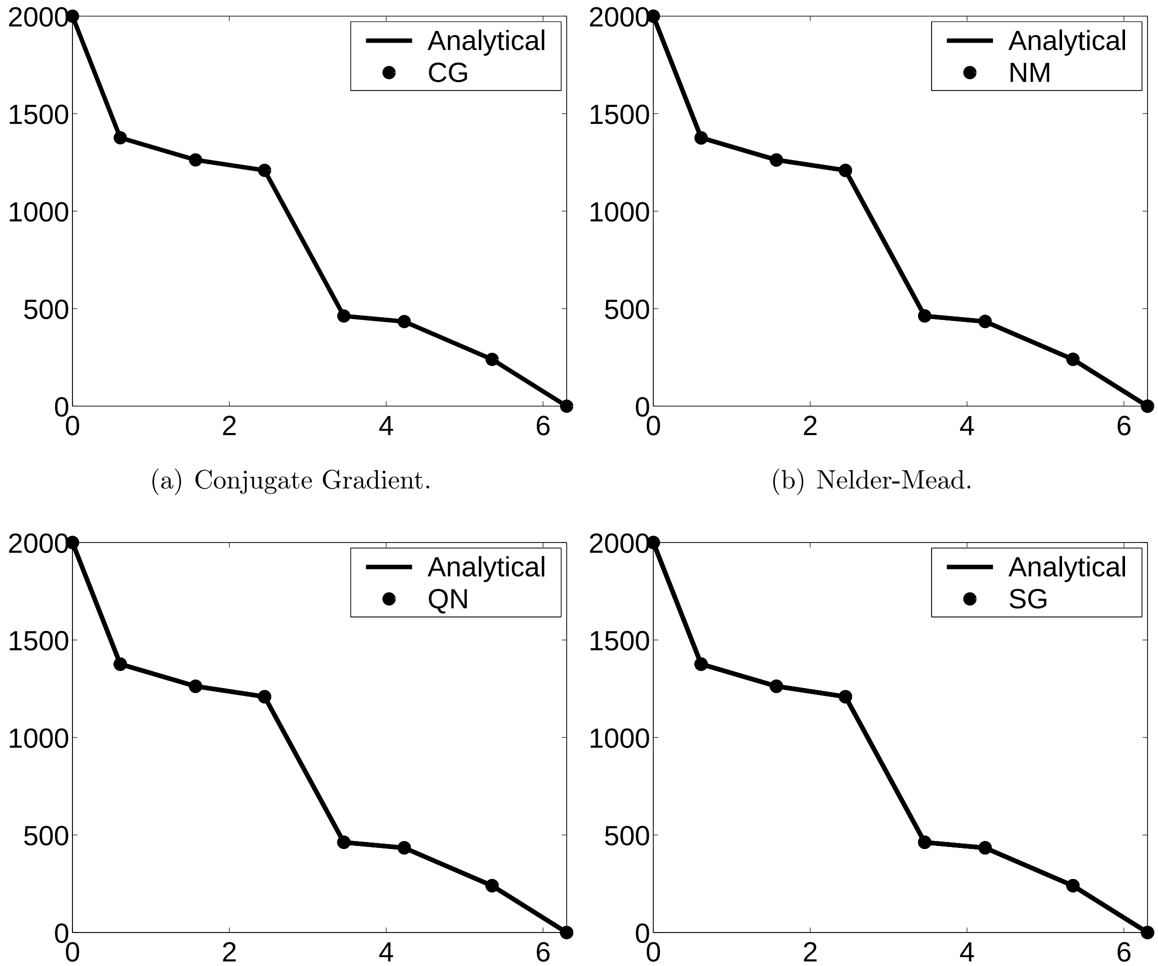

(a) Conjugate Gradient.

(b) Nelder-Mead.

(c) Quasi-Newton.

(d) Stochastic Global.

Figure 5: Comparison between the analytical solution and the solutions obtained from the indicated global optimization algorithms which are based on the energy minimization principle for the flow of a Newtonian fluid with $\mu = 0.15$ Pa.s. The computations were carried out using the 1D linear annular network of Table 5 with inlet and outlet pressures of 2000 Pa and 0 Pa respectively. The volumetric flow rate through the network is 2.120×10^{-5} $m^3.s^{-1}$. In all four sub-figures, the vertical axis represents the network axial pressure in Pa while the horizontal axis represents the network axial coordinate in m.

4 Non-Newtonian Flow in Elliptical Geometry

In [7] we demonstrated energy minimization in the flow of generalized Newtonian fluids (which include Newtonian and 6 non-Newtonian fluid types) through tubes and networks of interconnected tubes of circular cross sections, while in § 3 of the present paper we demonstrated energy minimization in the flow of Newtonian fluids through various cross sectional geometries (namely elliptical, rectangular, equilateral triangular, and concentric circular annular). In the present section we combine these two variations (i.e. the variation of fluid type and the variation of cross sectional geometry) by demonstrating energy minimization in the flow of non-Newtonian fluids (namely power law, Ellis and Ree-Eyring fluids) through tubes of elliptical cross sectional geometry.

In this regard we use the analytical expressions of Table 6 (as given in [18–20]) for the volumetric flow rate of power law, Ellis and Ree-Eyring fluids through tubes and networks of interconnected tubes of elliptical cross sectional geometry where the coordinate and parametric setting of the elliptical geometry with regard to these expressions is illustrated in Figure 1.

We conducted thorough investigations and computations of non-Newtonian fluid flow through elliptical tubes and networks (i.e. of interconnected elliptical tubes) of various dimensionality (i.e. 1D, 2D and 3D) and topology (such as linear, fractals, and irregulars based on cubic and orthorhombic lattices) using the three aforementioned non-Newtonian fluid types (i.e. power law, Ellis and Ree-Eyring) of various characteristics and parameters. All these investigations and computations lead to the definite conclusion that energy minimization holds in all these cases regardless of the type of elliptical vessel (i.e. whether single tube or network of interconnected tubes), regardless of the dimensionality and topology of network, and regardless of the characteristics and parameters of fluid.

A sample of these investigations and computations for some 1D linear networks (see Tables 7-9) are given in Figures 6-8, i.e. Figure 6 for the flow of a power law fluid through elliptical geometry, Figure 7 for the flow of an Ellis fluid through elliptical geometry, and Figure 8 for the flow of a Ree-Eyring fluid through elliptical geometry. The use of 1D linear networks in this sample demonstration is because of the ease of displaying and clarity of showing and interpreting the results of this type of networks which can be easily displayed on 2D plots (as seen in Figures 6-8) and clearly analyzed and interpreted.

As we see, this representative sample shows that the solutions that we obtained from the employment of the principle of energy minimization are virtually identical to the Poiseuille-type analytical solutions (as outlined in § 2). So, we can conclude with certainty that the

Table 6: The three types of generalized Newtonian fluid models and the volumetric rates Q for their flow through tubes of elliptical cross sectional geometry. The meanings of the symbols are given in § Nomenclature with reference to Figure 1 $\left(\text{noting that } A = \frac{\partial p}{\partial z}\frac{1}{a^2+b^2}\right)$. See [18–20].

Fluid Type	**Volumetric Flow Rate (Q)**
Power Law	$Q = \frac{4\arctan\left(\frac{\tan(\pi/2)}{\sqrt{1-e^2}}\right)}{\sqrt{1-e^2}}\left(\frac{\partial p}{\partial z}\frac{b^2}{k(a^2+b^2)}\right)^{1/n}\frac{n}{n+1}\left[\frac{nb^{(3n+1)/n}}{(3n+1)(1-e^2)^{(n+1)/(2n)}} - \frac{a^{(n+1)/n}b^2}{2}\right]$
Ellis	$Q = \left\{Ab^4\left[\frac{b^2}{2(1-e^2)} - a^2\right] + \frac{4A^\alpha b^{2\alpha+2}}{\tau_h^{\alpha-1}(\alpha+1)}\left[\frac{b^{\alpha+1}}{(1-e^2)^{(\alpha+1)/2}(\alpha+3)} - \frac{a^{\alpha+1}}{2}\right]\right\}\frac{\arctan\left(\frac{\tan(\pi/2)}{\sqrt{1-e^2}}\right)}{\mu_e\sqrt{1-e^2}}$
Ree-Eyring	$Q = \frac{4\tau_c^4\sqrt{1-e^2}}{A^3b^6\mu_0}\left[\frac{Ab^3}{\tau_c\sqrt{1-e^2}}\sinh\left(\frac{Ab^3}{\tau_c\sqrt{1-e^2}}\right) - \cosh\left(\frac{Ab^3}{\tau_c\sqrt{1-e^2}}\right) - \frac{A^2b^6}{2\tau_c^2(1-e^2)}\cosh\left(\frac{Ab^2a}{\tau_c}\right) + 1\right]\arctan\left(\frac{\tan(\pi/2)}{\sqrt{1-e^2}}\right)$

principle of energy minimization holds in general (i.e. independent of the type of vessel, the dimensionality and topology of network, and the type of generalized Newtonian fluid).

Table 7: The semi-major axes a, semi-minor axes b and lengths L of the seven elliptical tubes of the 1D linear network of Figure 6 as well as the pressure drops Δp across them. All numbers are in SI units (i.e. meters and pascals).

a	0.017, 0.023, 0.019, 0.021, 0.018, 0.024, 0.022
b	0.013, 0.017, 0.016, 0.016, 0.014, 0.019, 0.015
L	0.7, 0.8, 0.9, 0.9, 1.0, 0.9, 0.8
Δp	599.22, 185.48, 365.89, 294.12, 631.30, 144.88, 279.11

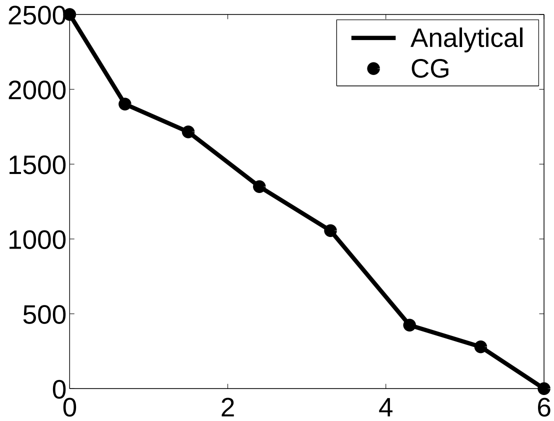

(a) Conjugate Gradient.

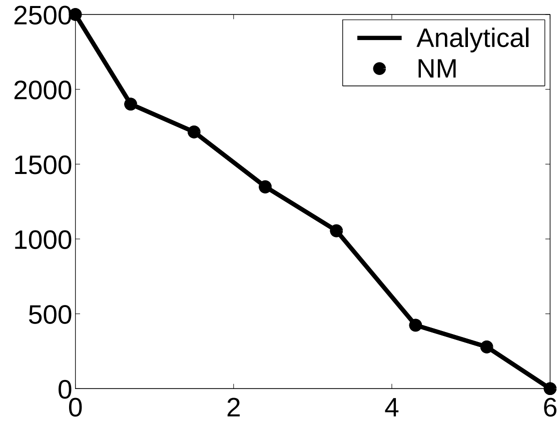

(b) Nelder-Mead.

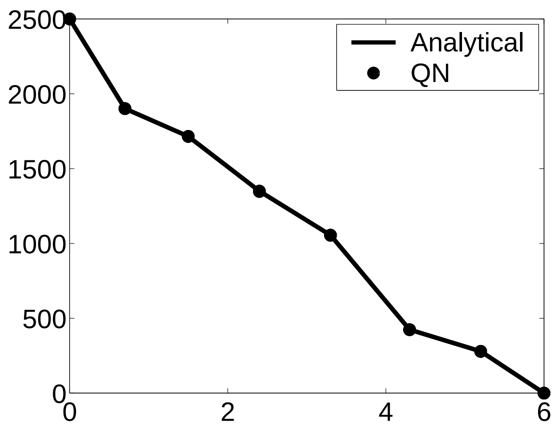

(c) Quasi-Newton.

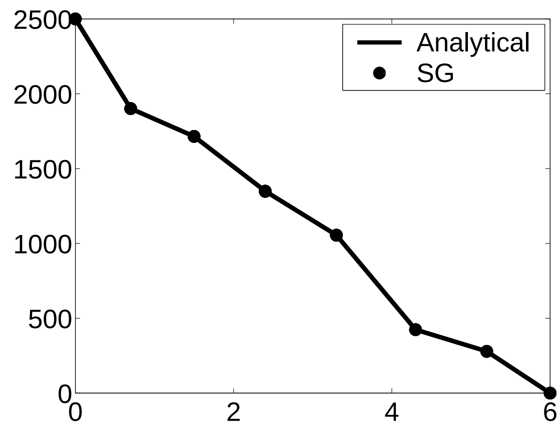

(d) Stochastic Global.

Figure 6: Comparison between the analytical solution and the solutions obtained from the indicated global optimization algorithms which are based on the energy minimization principle for the flow of a power law fluid with $n = 1.2$ and $k = 0.07$ Pa.s^n. The computations were carried out using the 1D linear elliptical network of Table 7 with inlet and outlet pressures of 2500 Pa and 0 Pa respectively. The volumetric flow rate through the network is 0.00011459 m^3.s^{-1}. In all four sub-figures, the vertical axis represents the network axial pressure in Pa while the horizontal axis represents the network axial coordinate in m.

Table 8: The semi-major axes a, semi-minor axes b and lengths L of the eight elliptical tubes of the 1D linear network of Figure 7 as well as the pressure drops Δp across them. All numbers are in SI units (i.e. meters and pascals).

a	0.0060, 0.0050, 0.0044, 0.0028, 0.0038, 0.0049, 0.0057, 0.0051
b	0.0046, 0.0035, 0.0034, 0.0024, 0.0029, 0.0041, 0.0045, 0.0047
L	0.024, 0.020, 0.024, 0.020, 0.028, 0.036, 0.028, 0.020
Δp	16.20, 34.16, 54.02, 197.90, 114.08, 44.66, 21.70, 17.28

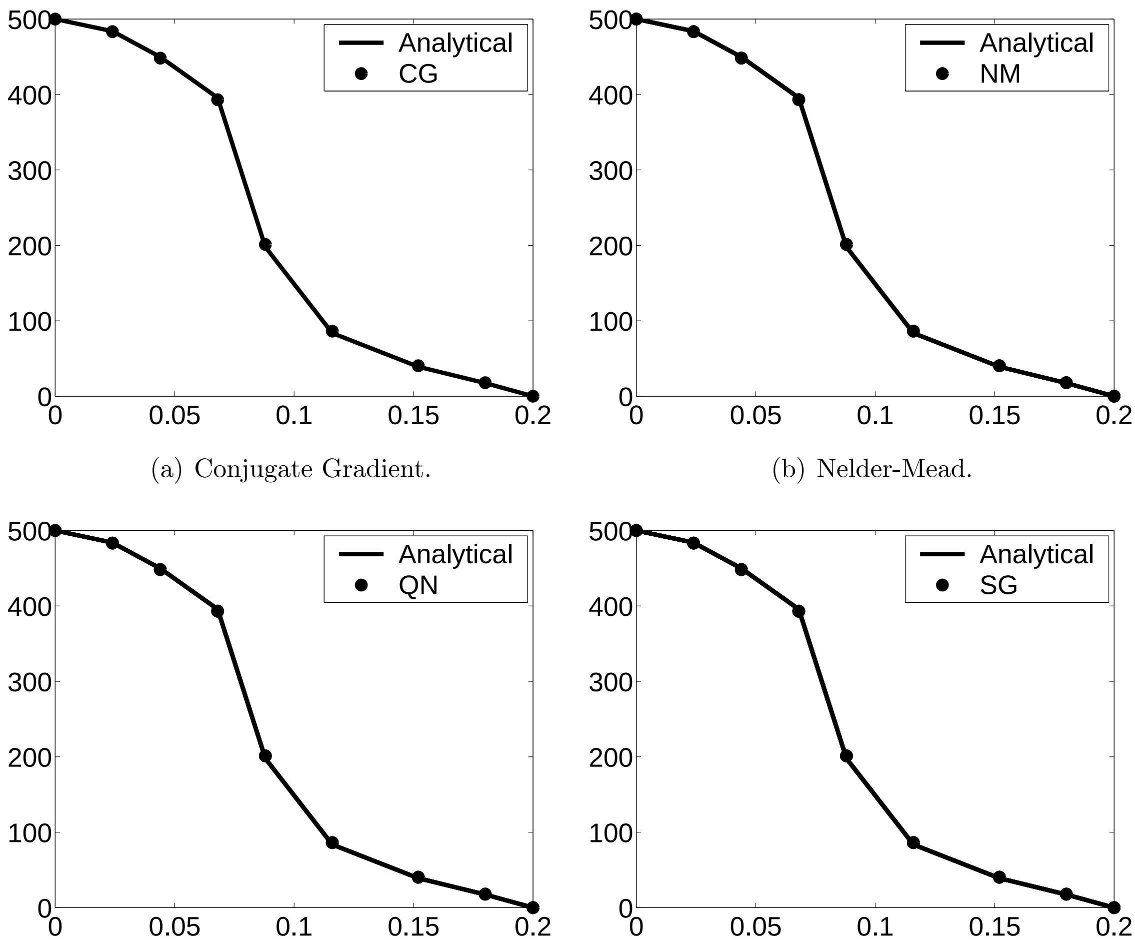

(a) Conjugate Gradient.

(b) Nelder-Mead.

(c) Quasi-Newton.

(d) Stochastic Global.

Figure 7: Comparison between the analytical solution and the solutions obtained from the indicated global optimization algorithms which are based on the energy minimization principle for the flow of an Ellis fluid with $\alpha = 2.4$, $\mu_e = 0.18$ Pa.s and $\tau_h = 40$ Pa. The computations were carried out using the 1D linear elliptical network of Table 8 with inlet and outlet pressures of 500 Pa and 0 Pa respectively. The volumetric flow rate through the network is 1.092×10^{-6} m^3.s^{-1}. In all four sub-figures, the vertical axis represents the network axial pressure in Pa while the horizontal axis represents the network axial coordinate in m.

Table 9: The semi-major axes a, semi-minor axes b and lengths L of the six elliptical tubes of the 1D linear network of Figure 8 as well as the pressure drops Δp across them. All numbers are in SI units (i.e. meters and pascals).

a	0.024, 0.020, 0.017, 0.022, 0.015, 0.018
b	0.021, 0.018, 0.015, 0.017, 0.014, 0.013
L	0.14, 0.08, 0.08, 0.14, 0.14, 0.17
Δp	87.34, 96.60, 188.52, 161.50, 469.82, 496.22

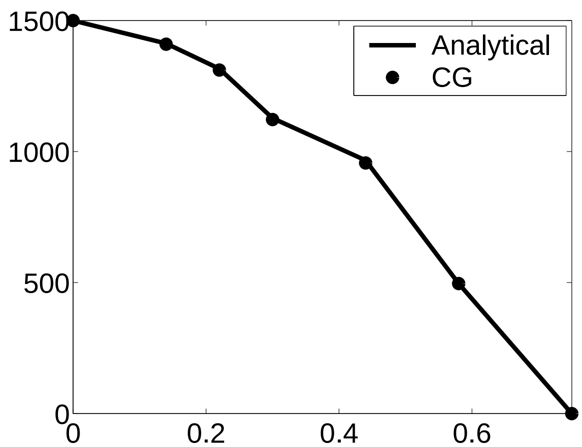

(a) Conjugate Gradient.

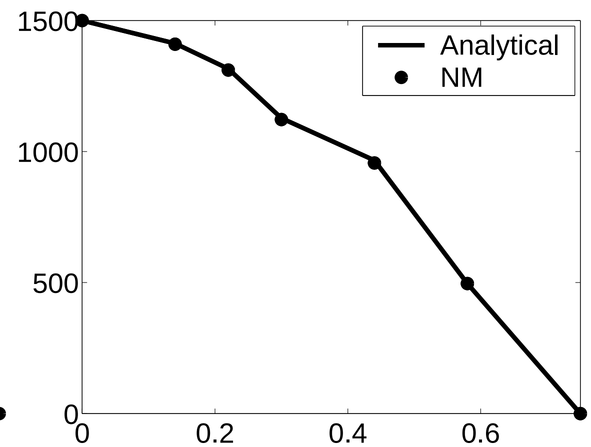

(b) Nelder-Mead.

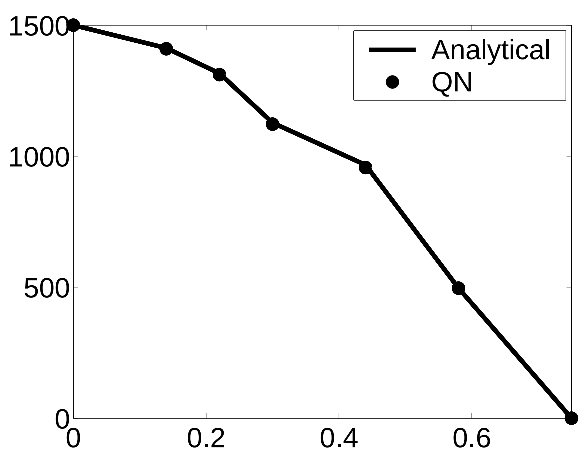

(c) Quasi-Newton.

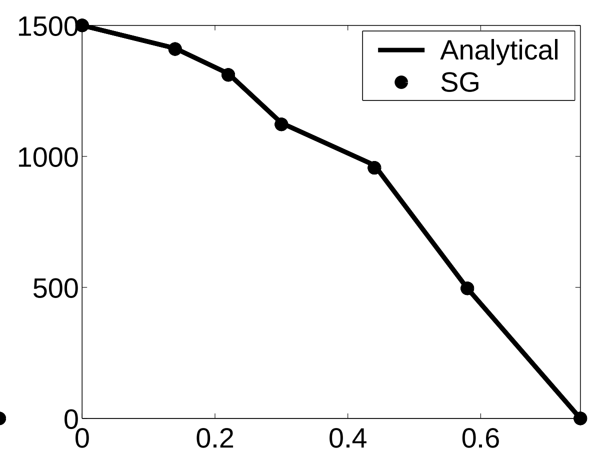

(d) Stochastic Global.

Figure 8: Comparison between the analytical solution and the solutions obtained from the global optimization algorithms which are based on the energy minimization principle for the flow of a Ree-Eyring fluid with $\mu_0 = 0.018$ Pa.s and $\tau_c = 30$ Pa. The computations were carried out using the 1D linear elliptical network of Table 9 with inlet and outlet pressures of 1500 Pa and 0 Pa respectively. The volumetric flow rate through the network is 0.0034445 $\mathrm{m}^3.\mathrm{s}^{-1}$. In all four sub-figures, the vertical axis represents the network axial pressure in Pa while the horizontal axis represents the network axial coordinate in m.

5 Conclusions

We outline in the following points the main achievements and conclusions of the present paper:

1. We continued our previous investigations about energy minimization in the flow of generalized Newtonian fluids through tubes and networks of interconnected tubes of various geometries. In the present study we extended and generalized the previous investigations by including non-circular and non-simply-connected geometries of tubes and networks of such tubes where we extended the investigation of this principle to the flow of Newtonian fluids through some of the common non-circular and non-simply-connected geometries (namely elliptical, rectangular, equilateral triangular and concentric circular annular geometries). We also extended this principle to the flow of three non-Newtonian fluid types (namely power law, Ellis and Ree-Eyring) through tubes and networks of interconnected tubes of elliptical cross sections.
2. All the results obtained in the current study support the generalization of the energy minimization as a fundamental principle that underlies the flow phenomena in the Newtonian and non-Newtonian fluid dynamics systems. The study also adds more tools to the subjects of Computational Fluid Dynamics (CFD) as these computational methods, which are based on energy minimization, can be used for finding the pressure and flow rate fields in tubes and networks and could have some advantages in some cases over the traditional methods (as indicated and concluded in our previous investigations).
3. The main conclusion of this investigation is that energy minimization in the flow of generalized Newtonian fluids through tubes and networks of interconnected tubes is general, i.e. it is independent of the type and geometry of the flow vessels and their topologies and it is independent of the type of fluids and their rheological properties. In fact, we may dare to say that energy minimization is a valid principle in all fluid dynamics systems regardless of the properties of vessels, fluids and flow conditions (i.e. within the restrictions and constraints of the particular fluid dynamics system and its physical conditions).
4. As well as its obvious theoretical value, the present investigation and the obtained results have practical values for the Computational Fluid Dynamics (as indicated already).
5. The relevance and usefulness of the present investigation and the obtained results extend beyond the subject of fluid flow through tubes and networks of interconnected tubes to include, for instance, the flow of fluids through porous media and the flow of electric currents through certain types of electrical networks such as networks of interconnected

ohmic conductors.

References

[1] C.D. Murray. The Physiological Principle of Minimum Work I. The Vascular System and the Cost of Blood Volume. *Proceedings of the National Academy of Sciences of the United States of America*, 12(3):207–214, 1926.

[2] C.D. Murray. The physiological principle of minimum work applied to the angle of branching of arteries. *The Journal of General Physiology*, 9(6):835–841, 1926.

[3] S. Rossitti; J. Löfgren. Vascular Dimensions of the Cerebral Arteries Follow the Principle of Minimum Work. *Stroke*, 24(3):371–377, 1993.

[4] A. Sharma; A. Al-Sarkhi; C. Sarica; H-Q Zhang. Modeling of oil-water flow using energy minimization concept. *International Journal of Multiphase Flow*, 37(4):326–335, 2011.

[5] T. Sochi. Solving the flow fields in conduits and networks using energy minimization principle with simulated annealing. 2014. arXiv:1408.0357.

[6] T. Sochi. Energy minimization for the flow in ducts and networks. 2014. arXiv:1412.1804.

[7] T. Sochi. Deterministic and stochastic algorithms for resolving the flow fields in ducts and networks using energy minimization. *International Journal of Modern Physics C*, 2014. DOI: 10.1142/S0129183116500364.

[8] T. Sochi. Using the Euler-Lagrange variational principle to obtain flow relations for generalized Newtonian fluids. *Rheologica Acta*, 53(1):15–22, 2014.

[9] T. Sochi. Variational approach for resolving the flow of generalized Newtonian fluids in circular pipes and plane slits. 2015. arXiv:1503.01262.

[10] A.H.P. Skelland. *Non-Newtonian Flow and Heat Transfer*. John Wiley & Sons Inc., 1967.

[11] R.B. Bird; R.C. Armstrong; O. Hassager. *Dynamics of Polymeric Liquids*, volume 1. John Wiley & Sons, second edition, 1987.

[12] F.M. White. *Viscous Fluid Flow*. McGraw Hill Inc., second edition, 1991.

[13] T.C. Papanastasiou; G.C. Georgiou; A.N. Alexandrou. *Viscous Fluid Flow*. CRC Press, first edition, 1999.

[14] T. Sochi. *Pore-Scale Modeling of Non-Newtonian Flow in Porous Media*. PhD thesis, Imperial College London, 2007.

[15] T. Sochi. Comparing Poiseuille with 1D Navier-Stokes Flow in Rigid and Distensible Tubes and Networks. 2013. arXiv:1305.2546.

[16] C.G.E. Boender; A.H.G. Rinnooy Kan; G.T. Timmer; L. Stougie. A stochastic method for global optimization. *Mathematical Programming*, 22(1):125–140, 1982.

[17] J. Lekner. Viscous flow through pipes of various cross-sections. *European Journal of Physics*, 28(3):521–527, 2007.

[18] T. Sochi. Flow of Power Law Fluids in Tubes of Elliptical Cross Sections. 2025. DOI: 10.26434/chemrxiv-2025-tcmc4.

[19] T. Sochi. Flow of Ellis Fluids in Tubes of Elliptical Cross Sections. 2025. DOI: https://doi.org/10.6084/m9.figshare.28282301.v1.

[20] T. Sochi. Flow of Ree-Eyring Fluids in Tubes of Elliptical Cross Sections. 2025. DOI: https://doi.org/10.6084/m9.figshare.28296173.v1.

Nomenclature

1D, 2D, 3D	one dimensional, two dimensional, three dimensional
a	length of side of equilateral triangle (m)
a, b	semi-major and semi-minor axes of ellipse (m)
a, b	semi-length and semi-width of rectangle (m)
a, b	outer and inner radii of concentric circular annulus (m)
e	eccentricity of ellipse ( )
Eq., Eqs.	Equation, Equations
I	time rate of energy consumption for fluid transport (J.s^{-1})
I_t	time rate of total energy consumption for fluid transport (J.s^{-1})

k	viscosity coefficient in the power law model (Pa.s^n)
L	tube length (m)
m	number of discrete/discretized elements in fluid conducting device ( )
n	flow behavior index in the power law model ( )
N	number of nodal junctions in fluid conducting device ( )
p	pressure (Pa)
Q	volumetric flow rate (m^3.s^{-1})
x, y, z	coordinate variables (usually spatial coordinates)
α	indicial parameter in Ellis model ( )
Δp	pressure drop across flow conduit (Pa)
μ	Newtonian viscosity (Pa.s)
μ_0	low-shear viscosity in Ree-Eyring model (Pa.s)
μ_e	low-shear viscosity in Ellis model (Pa.s)
τ_c	characteristic shear stress in Ree-Eyring model (Pa)
τ_h	shear stress when viscosity equals $\frac{\mu_e}{2}$ in Ellis model (Pa)